



OPEN ACCESS

EDITED BY

Jeremie Oliver Piña,
National Institutes of Health (NIH),
United States

REVIEWED BY

Shaohua Chen,
Beijing Institute of Technology, China
Zheng Duanmu,
Beijing Information Science and
Technology University, China

*CORRESPONDENCE

Yan Dong,
✉ dongyangx2022@126.com

RECEIVED 23 June 2023

ACCEPTED 10 October 2023

PUBLISHED 26 October 2023

CITATION

Zhang J, Liu C and Dong Y (2023), Finite element analysis of sagittal screw expander appliance in the treatment of anterior maxillary hypoplasia. *Front. Bioeng. Biotechnol.* 11:1245764. doi: 10.3389/fbioe.2023.1245764

COPYRIGHT

© 2023 Zhang, Liu and Dong. This is an open-access article distributed under the terms of the [Creative Commons Attribution License \(CC BY\)](https://creativecommons.org/licenses/by/4.0/). The use, distribution or reproduction in other forums is permitted, provided the original author(s) and the copyright owner(s) are credited and that the original publication in this journal is cited, in accordance with accepted academic practice. No use, distribution or reproduction is permitted which does not comply with these terms.

Finite element analysis of sagittal screw expander appliance in the treatment of anterior maxillary hypoplasia

Jian Zhang¹, Caiyun Liu² and Yan Dong^{1*}

¹College of Stomatology, Dalian Medical University, Dalian, Liaoning, China, ²Affiliated Hospital of Stomatology, Dalian Medical University, Dalian, Liaoning, China

The skeletal anterior crossbite is a common malocclusion in clinic. However, there have been no reports on the maxillary sagittal expansion to correct the premaxillary hypoplasia, which greatly influences the facial morphology and masticatory function, using finite element analysis. In the present study, a three-dimensional finite element model of craniomaxillofacial complex with maxillary sagittal hypoplasia is constructed and the treatment for premaxillary hypoplasia by the sagittal screw expander appliance is simulated. The hypoplasia of the left premaxilla is more serious than that of the right and thus the size of the left part of premaxillary expander baseplate is designed to be larger than that of the right part and the loading is applied at 10° leftward to the sagittal plane and 30° forward and downward to the maxillary occlusal plane. The displacements or equivalent stress distributions of the maxilla, teeth and their periodontal ligaments, are analyzed under the loads of 5.0 N, 10.0 N, 15.0 N, and 20.0 N. Consequently, as the load increases, the displacements or equivalent stresses of the maxilla, teeth and their periodontal ligaments all increase. Almost the whole premaxilla markedly move forward, downward, and leftward while other areas in the craniomaxillofacial complex remain almost static or have little displacement. The equivalent stress concentration zone of the maxilla mainly occurs around and in front of the incisive foramina. The displacements of left premaxilla are generally greater than those of the right under the loading forces. The maximum equivalent stress on the teeth and their periodontal ligaments are 2.34E-02 MPa and 2.98E-03 MPa, respectively. Taken together, the sagittal screw expander appliance can effectively open the premaxillary suture to promote the growth of the premaxilla. An asymmetrical design of sagittal screw expander appliance achieves the asymmetric expansion of the premaxilla to correct the uneven hypoplasia and obtains the more symmetrical aesthetic presentation. This study might provide a solid basis and theoretical guidance for the clinical application of sagittal screw expander appliance in the efficient, accurate, and personalized treatment of premaxillary hypoplasia.

KEYWORDS

finite element analysis, anterior maxillary hypoplasia, sagittal screw expander appliance, displacement, stress distribution

Introduction

The skeletal anterior crossbite is a common malocclusion in clinic (Lombardo et al., 2020; De Ridder et al., 2022), which mainly induced by hypoplasia of the maxilla, macroplastia of the mandible, or both (Zhang et al., 2023). For sagittal maxillary hypoplasia, orthopedic force is generally applied by the protraction appliance and transmitted to the sutural tissues in the craniomaxillofacial complex such as zygomaticomaxillary, pterygopalatine, zygomaticotemporal and frontomaxillary sutures to effectively promote the sagittal growth of the maxilla and correct the malocclusion relationship between the upper and lower dental arches (Matsumoto and Tanna, 2021; Vracar et al., 2021; Kamath et al., 2022; Wang et al., 2022). However, this treatment only can promote the sagittal growth of the posterior maxilla, but not the anterior, which greatly influences the facial morphology and masticatory function.

The premaxilla, where the four maxillary incisors are (WOO, 1949; Barteczko and Jacob, 2004), is closely associated with the development of the human facial morphology and is delimited by a suture that goes from the incisive foramina to the region between the lateral incisors and canines (Lisson and Kjaer, 1997). This suture goes down from the junction of the maxillary and premaxillary growth centers, near the lower portion of the pyriform aperture, to the alveolar margin of the canines, crossing the palate to the incisive foramina. Trevizan et al. (2018) analyzed the premaxillary sutures in 1138 human dry skulls and found that all sutures gradually closed at a rate of 3.72% per year from birth to 12 years old and were not fully closed at the age of 12 yet. Therefore, during the peak and pre-peak growth periods of children, the premaxillary suture can be opened by expander appliance to promote the growth of premaxilla, which can correct the hypoplasia of the anterior maxilla effectively.

Up to now, finite element analyses on the treatment of maxillary hypoplasia have mainly focused on the protraction (Garg et al., 2023), transverse expansion of the maxilla (Fernandes et al., 2021), and the interaction between them (Balakrishnan et al., 2023). Although clinically, a sagittal screw expander appliance placed on the palate of the maxilla is used to open the premaxillary suture (Farronato et al., 2011; Maspero et al., 2020), there have been no reports on the analysis of sagittal screw expander appliance in the treatment for the anterior maxillary hypoplasia using the finite element method. The purpose of this study is to investigate the effects of sagittal screw expander appliance on the anterior maxillary hypoplasia by finite element analysis, providing the potent basis for the clinical treatment of premaxillary hypoplasia.

Materials and methods

The finite element model of the craniomaxillofacial complex, consisting of bones, sutures, teeth, and periodontal ligaments, is constructed from the Cone-Beam Computed Tomography (CBCT) images of a 9-year-old boy with skeletal anterior crossbite at the mixed dentition stage by using MIMICS 19.0 (Materialise, Leuven, Belgium), Geomagic Wrap 2017 (Geomagic Inc., Utah, United States of America), and Ansys 18.2 (ANSYS Inc., Canonsburg, PA) (Figures 1A, B). In the model, hypoplasia of the left anterior maxilla is more severe than that of the right. The width of the periodontal ligament and premaxillary suture is 0.2 mm (Kojima and Fukui, 2006), and the other maxillofacial sutures is 0.5 mm wide (Fricke-Zech et al., 2012).

The computer aided design (CAD) model of the sagittal screw expander appliance with resin baseplate of an average thickness of 2.0 mm and stainless steel clasp of a diameter of 0.8 mm is

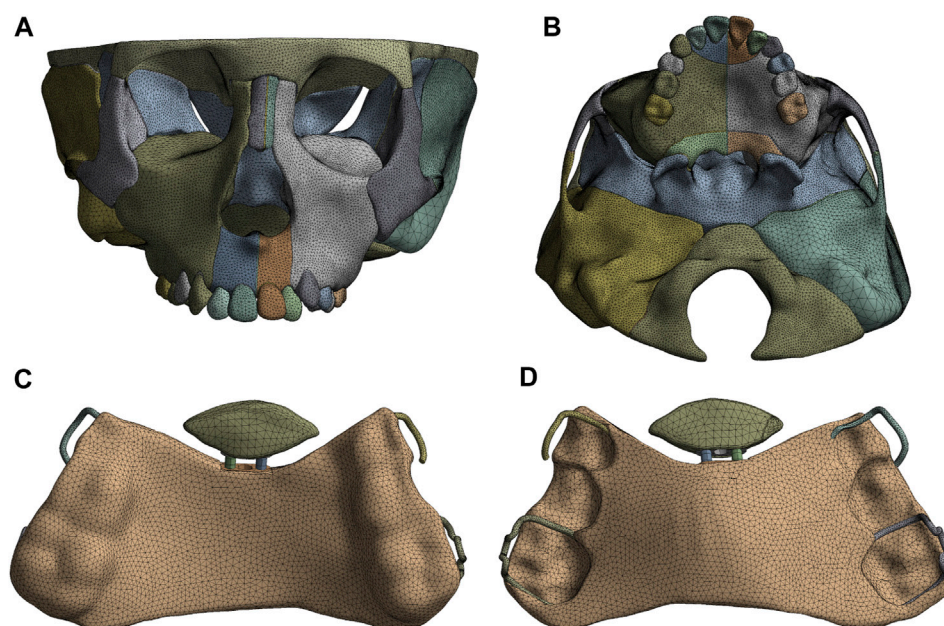


FIGURE 1
The finite element model of craniomaxillofacial complex (A), Frontal view; (B), Palatal view and sagittal screw expander appliance (C), Lingual view; (D), Palatal view.

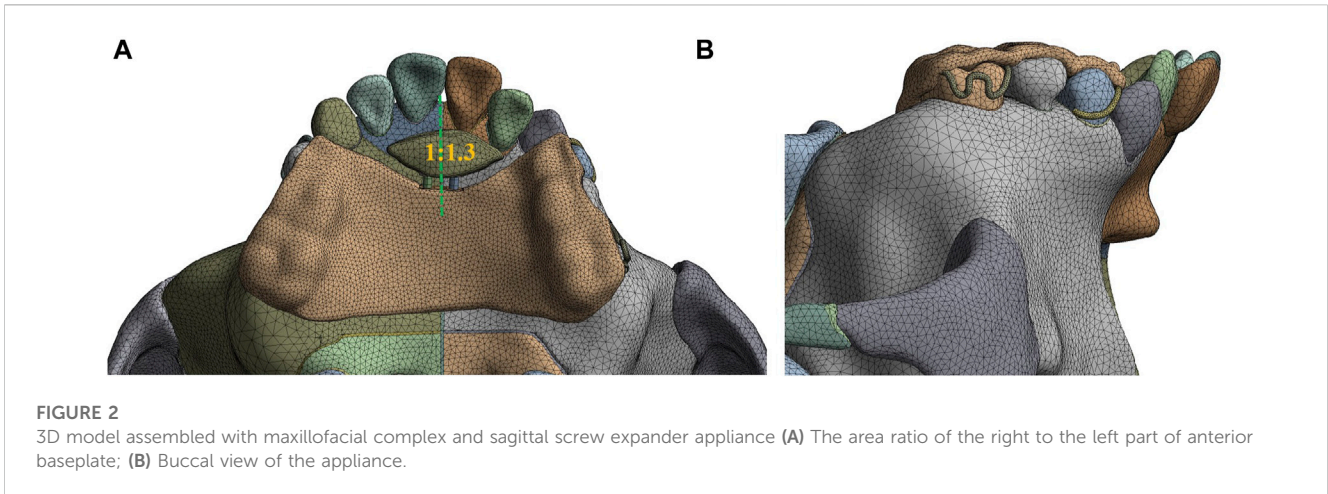


FIGURE 2
3D model assembled with maxillofacial complex and sagittal screw expander appliance (A) The area ratio of the right to the left part of anterior baseplate; (B) Buccal view of the appliance.

TABLE 1 The Young’s moduli and Poisson’s ratios for all materials.

Material	Young’s modulus (MPa)	Poisson’s ratios
Bone	10000	0.3
Suture	0.68	0.47
Tooth	18600	0.31
Periodontal ligament	68.9	0.45
Steel	200000	0.3
Baseplate	4500	0.35

established by using Solidworks 2020 (Dassault Systems, Concord, MA) (Figures 1C,D). The anterior baseplate is placed on the palate of the premaxilla and the area of the left part of anterior baseplate is 1.3 times larger than that of the right (Figure 2A). The posterior baseplate is connected to the occlusal splint, and to prevent premature loss of the maxillary second deciduous molars with obvious root resorption, the occlusal splint does not come into contact with them. The clasps are placed on the crowns of the first premolar and first molar of the maxilla as shown in Figure 2B.

The finite element model assembled from the craniomaxillofacial complex and sagittal screw expander appliance models consists of 1,002,520 elements ranging in size from 0.3 to 1.0 mm and 1,151,917 nodes. Furthermore, the materials involved are all assumed to be continuous, homogeneous, and isotropic linear elastic, with Young’s moduli and Poisson’s ratios shown in Table 1 (Weinstein et al., 1980; Serpe et al., 2014; Tanaka et al., 2015; Zarrati et al., 2015; Li et al., 2020; Duanmu et al., 2021; Sujaritwanid et al., 2021).

The three-dimensional coordinate system is defined by the occlusal plane as the X-axis (sagittal), Y-axis (vertical), and Z-axis (coronal). Positive values represent backward, upward, and leftward displacements on the X, Y, and Z-axis, respectively. The expansion screw is activated by loads of 5.0 N, 10.0 N, 15.0 N, and 20.0 N at 30° forward and downward to the maxillary occlusal plane and 10° leftward to the sagittal plane, and the foramen magnum is fixed (Figure 3) (Ge et al., 2012; Lee and Baek, 2012; Lee et al., 2016; Shyagali et al., 2023). As shown in Figure 4, ten landmarks include

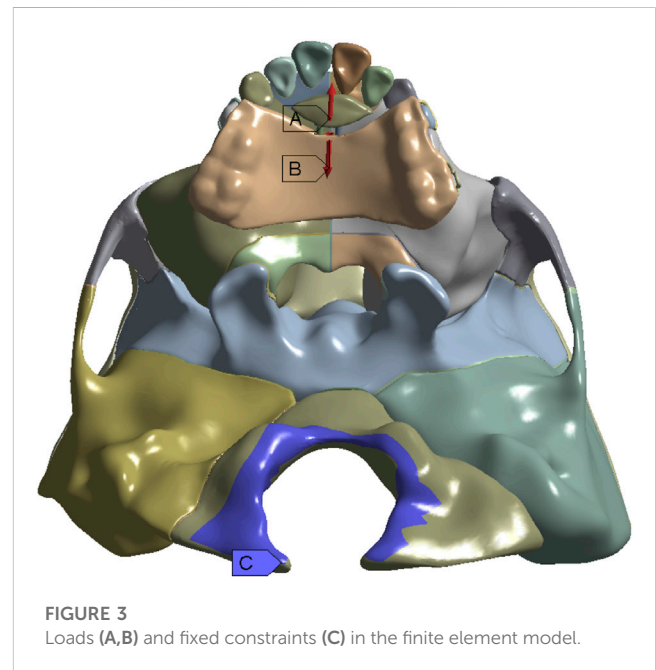


FIGURE 3
Loads (A,B) and fixed constraints (C) in the finite element model.

incisive foramen points (a,b), lateral incisor palatal points (c,d), symmetrical points of incisive foramina with the premaxillary suture as the symmetry axis (e,f), canine palatal points (g,h), and the A. subspinales (i,j).

By using Ansys 18.2 (ANSYS Inc., Canonsburg, PA), the displacements on the X, Y, Z-axis of ten landmarks and maxilla, the total displacement and equivalent stress distribution of the maxilla, and the equivalent stress distributions of the maxillary first premolars, first molars and their periodontal ligaments, are analyzed under the four loads of 5.0 N, 10.0 N, 15.0 N, and 20.0 N.

Results

As the load increases from 5.0 N to 20.0 N, the absolute displacement values of all landmarks in the X-axis direction increase. The landmarks on the premaxilla (A.subspinales,

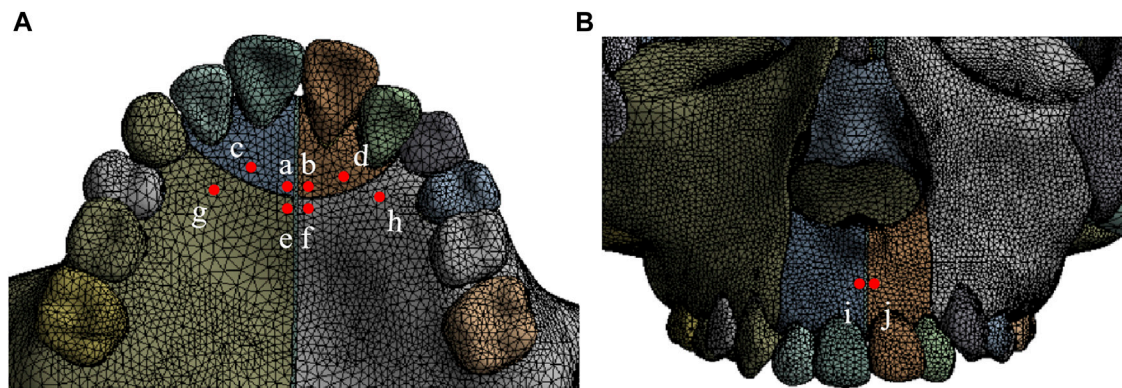


FIGURE 4

Ten landmarks on the anterior maxilla (A) ab, incisive foramen; cd, lateral incisor palatal point; ef, symmetrical point of incisive foramen; gh, canine palatal point; (B) ij, A.subspinale.

TABLE 2 Displacements of landmarks in the X-axis direction (mm).

Landmarks		Load			
		5.0 N	10.0 N	15.0 N	20.0 N
Incisive foramen point	Left	-9.46E-05	-1.89E-04	-2.84E-04	-3.78E-04
	Right	-8.70E-05	-1.74E-04	-2.61E-04	-3.48E-04
Lateral incisor palatal point	Left	-1.16E-04	-2.33E-04	-3.49E-04	-4.65E-04
	Right	-9.64E-05	-1.93E-04	-2.89E-04	-3.85E-04
A.subspinale	Left	-8.64E-06	-1.73E-05	-2.59E-05	-3.45E-05
	Right	-4.47E-07	-8.95E-07	-1.34E-06	-1.79E-06
Symmetrical point of incisive foramen	Left	1.39E-05	2.78E-05	4.17E-05	5.56E-05
	Right	1.93E-05	3.87E-05	5.80E-05	7.73E-05
Canine palatal point	Left	7.12E-06	1.42E-05	2.13E-05	2.85E-05
	Right	5.39E-06	1.08E-05	1.62E-05	2.15E-05

incisive foramen points, and lateral incisor palatal points) move forward and the absolute displacement values of landmarks on the left premaxilla are all greater than those on the right. When the load is 20.0 N, the forward movement distances of the left/right incisive foramen point and lateral incisor palatal point, are 3.78E-04/3.48E-04 mm, 4.65E-04/3.85E-04 mm, respectively. On the maxilla region behind the premaxillary suture, the symmetrical points of incisive foramina and canine palatal points have little displacement (Table 2).

As the load increases, the absolute displacement values of ten landmarks in the Y-axis direction become larger, and all landmarks move downward except for the symmetrical points of incisive foramina. When the load is 20.0 N, the downward movement distances of the left/right incisive foramen point, lateral incisor palatal point, and A. subspinale are 4.94E-04/4.61E-04 mm, 4.01E-04/3.59E-04 mm, and 1.26E-04/1.15E-04 mm, respectively. The symmetrical points of incisive foramina and canine palatal points behind the premaxillary suture remain almost static (Table 3).

As the load increases, in the Z-axis direction, displacements of ten landmarks increase. The displacements of landmarks on the left premaxilla are significantly greater than those of the corresponding landmarks on the right except for the A. subspinale. When the load is 20.0 N, displacements of the left incisive foramen point and lateral incisor palatal point are 1.47E-04 mm and 1.41E-04 mm, respectively, while the right corresponding ones, A. subspinale, symmetrical points of incisive foramina and canine palatal points all have little displacement (Table 4).

Furthermore, we investigate displacements in the X, Y, and Z-axis directions and the total displacement of the maxilla, which all increase as the load increases. In the X-axis direction, most of the premaxilla moves forward and the greatest displacement, 5.61E-04 mm, occurs in the palatal alveolar process of left lateral incisor (Figure 5). In the Y-axis direction, as shown in Figure 6, most of the premaxilla moves downward and the largest displacement appears around the incisive foramina. On the Z-axis, the left premaxilla has a remarkable leftward movement (Figure 7), and the maximum movement distance, 1.74E-04 mm, occurs in the palatal alveolar

TABLE 3 Displacements of landmarks in the Y-axis direction (mm).

Landmarks		Load			
		5.0 N	10.0 N	15.0 N	20.0 N
Incisive foramen point	Left	-1.23E-04	-2.47E-04	-3.70E-04	-4.94E-04
	Right	-1.15E-04	-2.30E-04	-3.45E-04	-4.61E-04
Lateral incisor palatal point	Left	-1.00E-04	-2.00E-04	-3.00E-04	-4.01E-04
	Right	-8.97E-05	-1.79E-04	-2.69E-04	-3.59E-04
A.subspinale	Left	-3.14E-05	-6.29E-05	-9.43E-05	-1.26E-04
	Right	-2.89E-05	-5.77E-05	-8.66E-05	-1.15E-04
Symmetrical point of incisive foramen	Left	4.61E-07	9.23E-07	1.38E-06	1.85E-06
	Right	1.16E-06	2.32E-06	3.48E-06	4.64E-06
Canine palatal point	Left	-9.87E-08	-1.97E-07	-2.96E-07	-3.95E-07
	Right	-1.59E-07	-3.17E-07	-4.76E-07	-6.35E-07

TABLE 4 Displacements of landmarks in the Z-axis direction (mm).

Landmarks		Load			
		5.0 N	10.0 N	15.0 N	20.0 N
Incisive foramen point	Left	3.68E-05	7.37E-05	1.10E-04	1.47E-04
	Right	1.05E-05	2.09E-05	3.14E-05	4.18E-05
Lateral incisor palatal point	Left	3.52E-05	7.04E-05	1.06E-04	1.41E-04
	Right	7.19E-06	1.44E-05	2.16E-05	2.88E-05
A.subspinale	Left	2.41E-06	4.82E-06	7.24E-06	9.65E-06
	Right	9.61E-06	1.92E-05	2.88E-05	3.85E-05
Symmetrical point of incisive foramen	Left	2.42E-06	4.85E-06	7.27E-06	9.70E-06
	Right	5.04E-06	1.01E-05	1.51E-05	2.02E-05
Canine palatal point	Left	2.10E-06	4.20E-06	6.30E-06	8.40E-06
	Right	9.25E-06	1.85E-05	2.77E-05	3.70E-05

process of the left lateral incisor, while the right premaxilla has little displacement. Figure 8 shows that under the loading forces, most of the premaxilla has obvious displacement while the maxillary region behind the premaxillary suture almost has no displacement, and the total displacements of the left premaxilla are generally greater than those of the right.

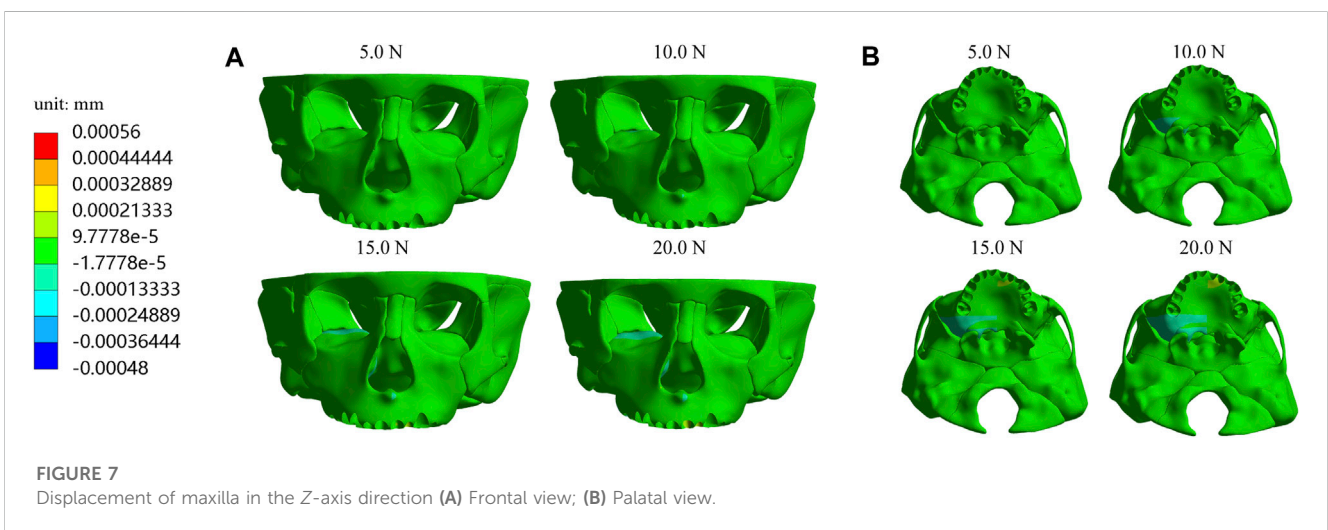
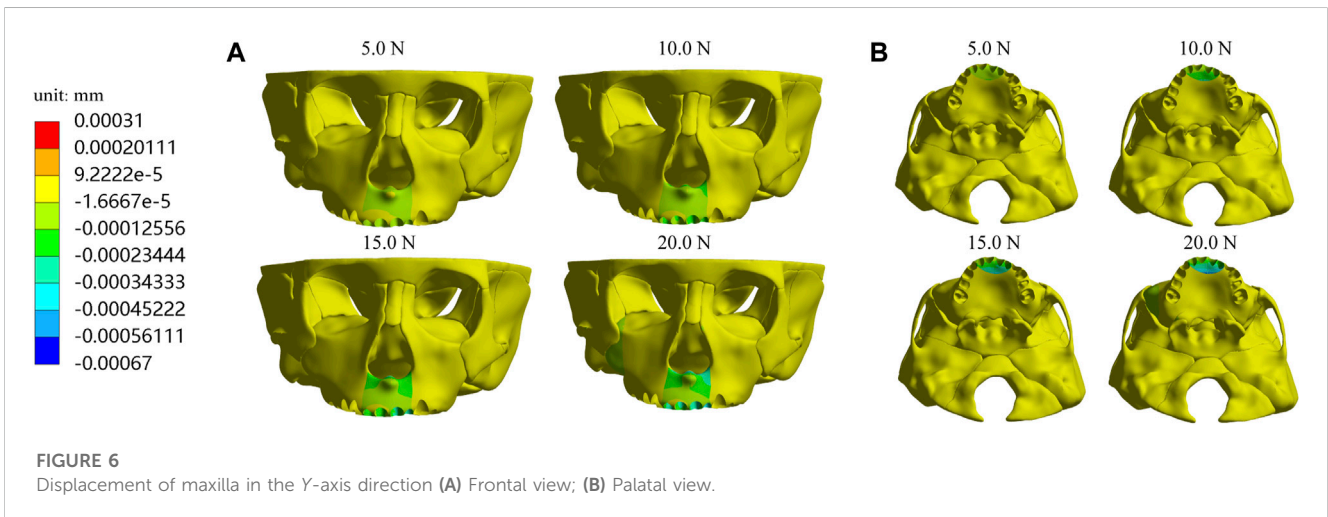
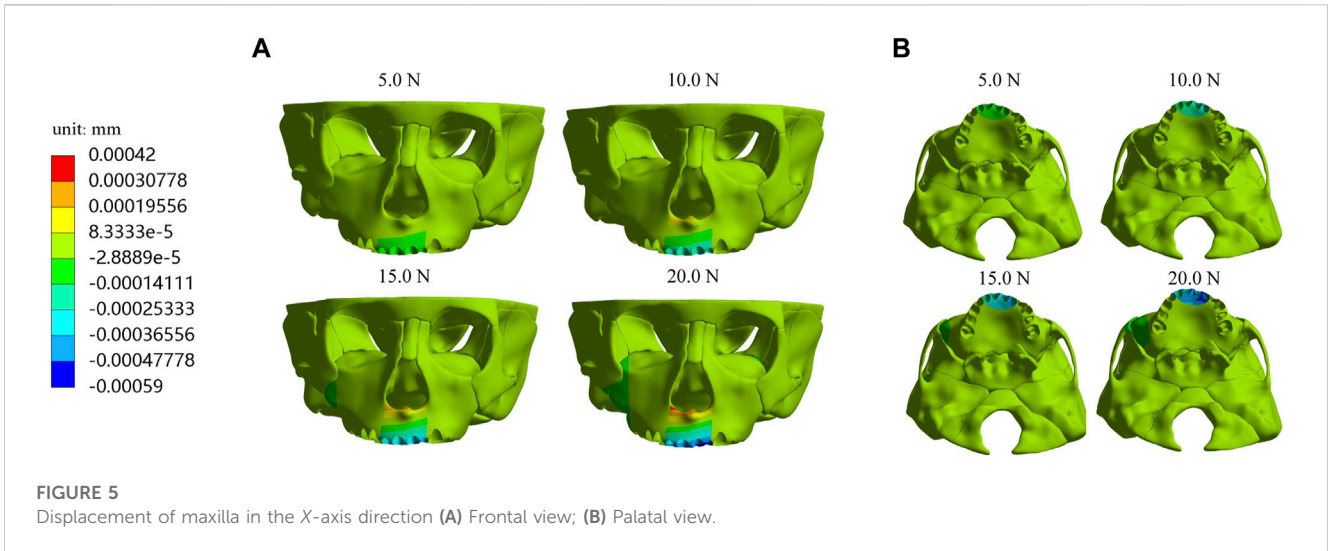
In addition, we analyze the equivalent stress on the maxilla, the first premolar, first molar and their periodontal ligaments under the four loads and the results showed that the equivalent stresses are enhanced when the load increases. The stress distributions on the maxilla and the profile of the premaxillary suture are shown in Figure 9, and it can be observed that the stress concentrations of the maxilla mainly occur in a large area around and in front of the incisor foramina. The largest stress concentration area of the teeth is located in the mesial region of the left first premolar crown (Figure 10A) and that of the periodontal ligament appears in the palatal cervical region of the left first premolar periodontal ligament

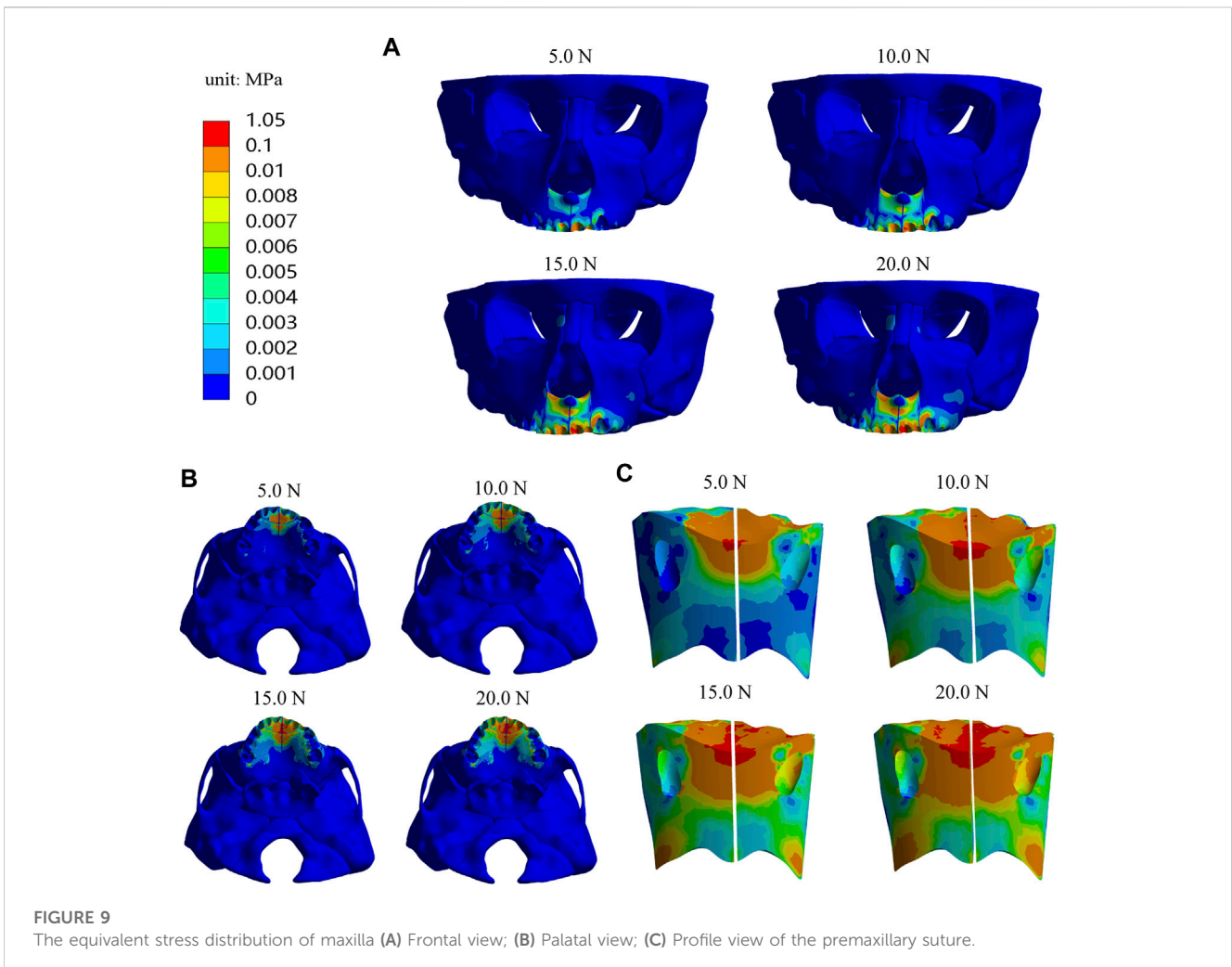
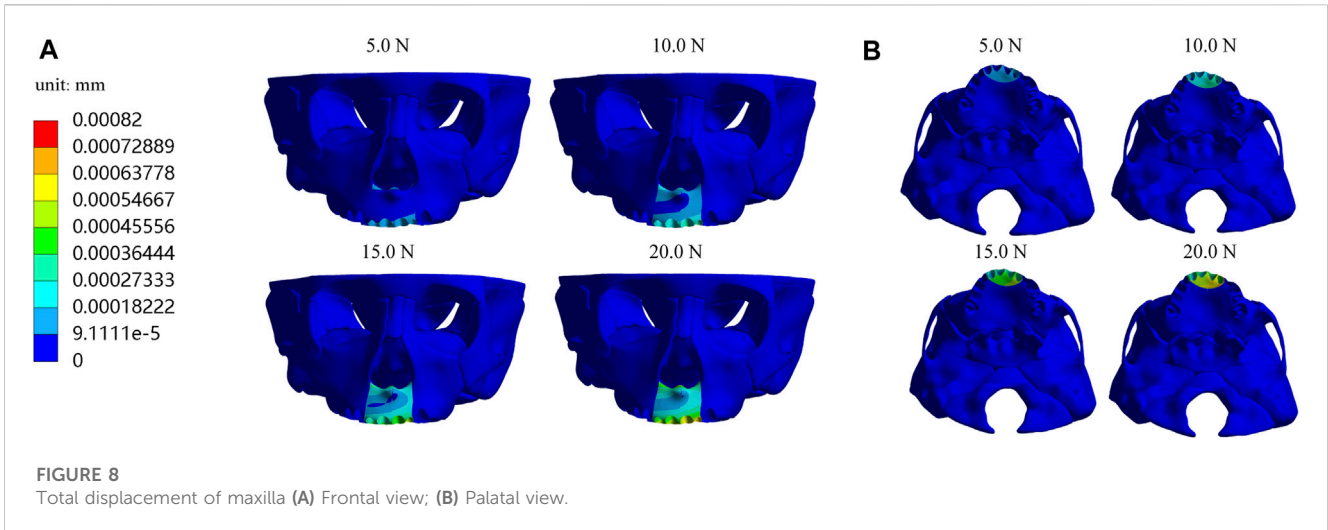
(Figure 10B). When the load is 20.0 N, the maximum equivalent stress are 2.34×10^{-2} and 2.98×10^{-3} MPa on the left maxillary first premolar and its periodontal ligament, respectively (Figures 10C,D).

Discussion

Nowadays, finite element analysis has been widely used in researches on the treatment of the different types of malocclusion. It can effectively simulate the orthodontics process and predict the treatment effects (Mitani et al., 2018; Choi et al., 2021; Maheshwari et al., 2023; Somaskandhan et al., 2023). However, there have been no reports on the analysis of maxillary sagittal expansion to correct the premaxilla hypoplasia using finite element method.

In the present study, three-dimensional finite element models of the craniomaxillofacial complex and sagittal screw expander





appliance are constructed and then the treatment of premaxillary hypoplasia is simulated. It is worth noting that the hypoplasia of the left premaxilla is more serious than that of the right, showing an asymmetric premaxillary hypoplasia. Some studies have indicated

that an asymmetric orthodontic appliance can effectively correct the asymmetry. Choi et al. (2021) employed a palatal asymmetric transverse expansion appliance and achieved differential displacements between the left and right maxilla using finite

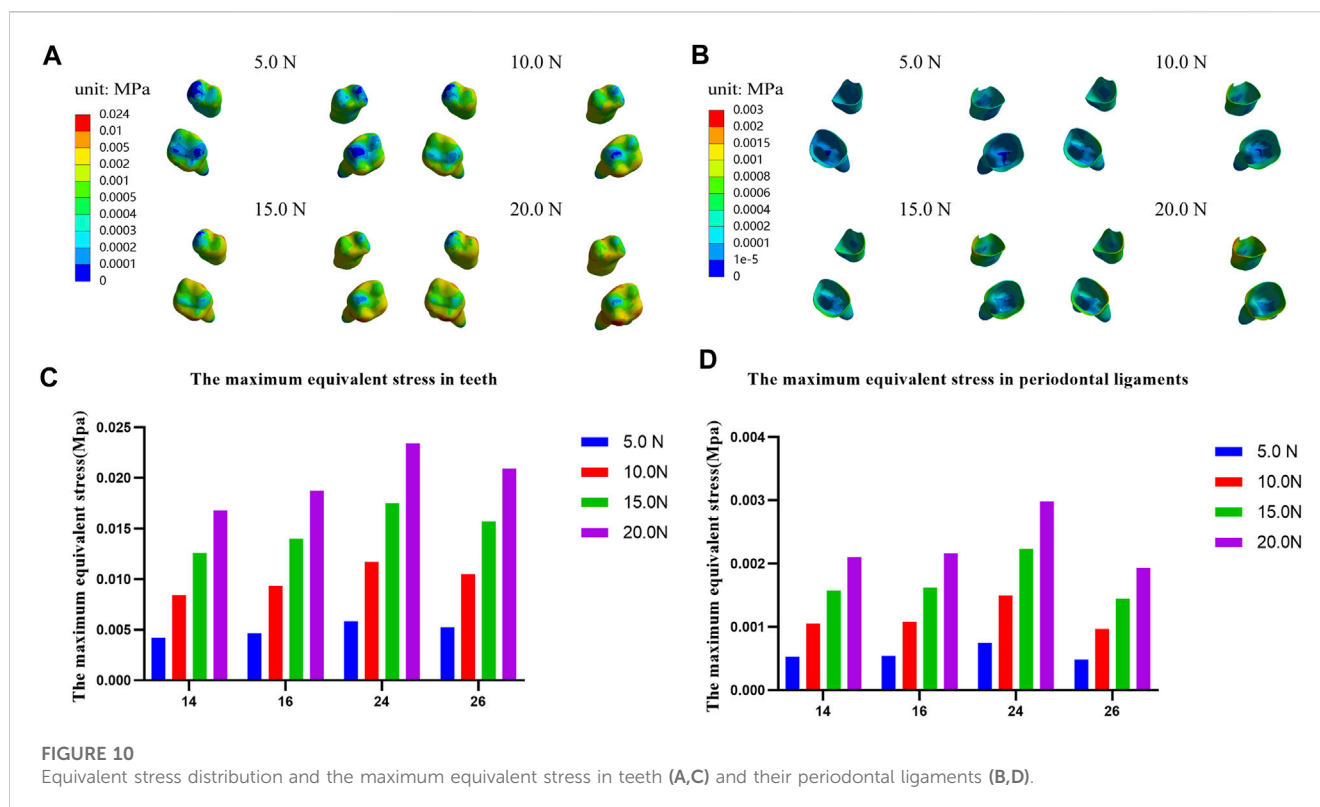


FIGURE 10 Equivalent stress distribution and the maximum equivalent stress in teeth (A,C) and their periodontal ligaments (B,D).

element analysis. Furthermore, in a clinical treatment for a 14-year-old girl with more severe hypoplasia in her left maxilla compared to the right, they used an asymmetric transverse expansion appliance with the larger left baseplate section. The clinical treatment results confirmed that when asymmetric maxillary needs to be corrected, asymmetric maxillary expansion could produce more symmetric orthodontic outcomes. Chen et al. (2015) used finite element analysis to apply asymmetrical loads in the treatment of a patient with asymmetrical maxillary hypoplasia induced by the unilateral cleft lip and palate. The results demonstrated that the asymmetric loading induced asymmetrical displacements of the left and right maxilla, achieving a more symmetrical appearance. Sadeghi et al. (2019) suggested that employing an asymmetric loading was effective in generating asymmetric distal movement of the molars.

In the present study, the hypoplasia of the left premaxilla is more severe than that of the right, so we designed the anterior baseplate to be asymmetric, with the left part of premaxillary expander baseplate being larger than the right part, and applied the loading forces at 10° leftward to the sagittal plane. Simulation results indicate that an asymmetric appliance can effectively generate a larger displacement and growth in the left maxilla. Under different magnitudes of orthopedic forces, the forward, leftward, and downward displacements of the left premaxillary landmark b and d are all greater than those of the corresponding right landmark a and c, respectively (Table 2–4), and the total displacements of the left premaxilla are generally greater than those of the right part (Figure 8). These results suggest that the asymmetric design of the maxillary expander is beneficial for correcting the asymmetric hypoplasia of the premaxilla.

As the load increases from 5.0 N to 20.0 N, the absolute displacement values of all landmarks in the X, Y, and Z-axis

directions increase (Table 2–4). In the X-axis direction, the landmarks (a, b, c, d) on the premaxilla all move forward, and their displacements reached the maximum under 20.0 N load, which are 3.48E-04, 3.78E-04, 3.85E-04, 4.65E-04 mm, respectively, while landmarks (e, f, g, h) located behind the premaxillary suture have little displacements. In the Y-axis direction, Point a, b, c, d, i, and j on the premaxilla all move downward significantly, and have the largest displacements under 20.0 N load, which are 4.61E-04, 4.94E-04, 3.59E-04, 4.01E-04, 1.15E-04, and 1.26E-04 mm, respectively, while Point e, f, g and h behind the premaxillary suture almost have no displacements. Taken together, it can be concluded that the loading forces applied in the direction with 30° forward and downward to the occlusal plane can cause the premaxilla to move forward and downward on the whole. Therefore, the sagittal screw expander appliance can open the premaxillary suture and hence effectively promote the growth of the premaxilla. In addition, A. subspinales have little forward displacements in the X-axis direction, so we plan to use the sagittal screw expander appliance in combination with the protraction to achieve further forward displacement of the whole maxilla in further research.

In the Z-axis direction, all the landmarks move left, which is due to the left part of the baseplate on the premaxilla being significantly larger than the right part and loading forces applied at 10° leftward to the sagittal plane. The results show that the maximum displacement values of landmark b and d on the left premaxilla are 1.47E-04 and 1.41E-04 mm, respectively, while the right premaxilla has remain almost static, which suggest that the leftward development of the left premaxilla with the more severe hypoplasia is promoted effectively.

In addition, the equivalent stress distribution and displacement of the maxilla are analyzed and from the stress distribution on the

maxilla and the profile of the premaxillary suture displayed in Figure 9, the equivalent stress concentration zone is mainly located in a large area around and in front of the incisive foramina, which indicates that orthopedic forces applied by the sagittal screw expander appliance are transmitted effectively to the premaxilla, contributing to the expansion of premaxillary suture. Interestingly, by the displacement analysis, we find that the premaxilla has obvious displacement and the maximum forward and leftward movement distances, $5.61\text{E-}04$ and $1.74\text{E-}04$ mm, respectively, appear in the region around the palatal alveolar process of the left lateral incisor with severe hypoplasia, suggesting that the premaxilla is accurately expanded by personalized design of sagittal screw expander appliance (Figures 5, 7, 8).

Moreover, we studied the equivalent stress distribution on the maxillary first premolars and first molars with the clasp and occlusal splint, and their periodontal ligaments. The results show that the equivalent stress increase with the increase of load. The maximum value on the teeth and the periodontal ligaments are $2.34\text{E-}02$ MPa and $2.98\text{E-}03$ MPa, respectively, on the left maxillary first premolar and its periodontal ligaments under 20.0 N load (Figure 10), which are far lower than the yield strength of the tooth (97.8 MPa) (Staninec et al., 2002) and the periodontal ligament (0.026 MPa) (Lee, 1965). Therefore, when the sagittal screw expander appliance is used to promote the growth of the premaxilla, it will not cause the tooth fracture and periodontal ligament injury.

Conclusion

The three-dimensional finite element models of craniomaxillofacial complex with sagittal maxillary hypoplasia and the sagittal screw expander appliance are successfully constructed and the treatment of the anterior maxillary hypoplasia by the sagittal screw expander appliance is simulated using CAD softwares. Under the orthopedic force ranged from 5.0 to 20.0 N, the screw expander appliance can open the premaxillary suture without causing the tooth fracture and periodontal ligament injury, and the greater the applied orthopedic force, the greater the opening of the premaxillary suture, which has suggested that sagittal expansion can effectively promote the growth of the premaxilla. Moreover, for the asymmetric anterior maxillary hypoplasia, we design an asymmetric appliance and achieve asymmetric expansion of the premaxilla to correct the uneven hypoplasia and obtain the more symmetrical aesthetic presentation. Taken together, this study might provide a solid basis and theoretical guidance for the clinical application of sagittal screw expander appliance in the efficient, accurate, and personalized treatment of premaxillary hypoplasia.

References

- Balakrishnan, R., Sengottuvel, N., Altaf, S. K., Bhandari, P. K., Kumaragurubaran, P., and Antony, M. (2023). Three-dimensional finite element analysis of maxillary protraction using diverse modes of rapid palatal expansion. *Cureus* 15 (3), e36328. doi:10.7759/cureus.36328
- Bartczko, K., and Jacob, M. (2004). A re-evaluation of the premaxillary bone in humans. *Anat. Embryol. Berl.* 207 (6), 417–437. doi:10.1007/s00429-003-0366-x
- Chen, Z., Pan, X., Zhao, N., Chen, Z., and Shen, G. (2015). Asymmetric maxillary protraction for unilateral cleft lip and palate patients using finite element analysis. *J. Craniofac Surg.* 26 (2), 388–392. doi:10.1097/SCS.0000000000001337
- Choi, J. Y., Choo, H., Oh, S. H., Park, J. H., Chung, K. R., and Kim, S. H. (2021). Finite element analysis of C-expanders with different vertical vectors of anchor screws. *Am. J. Orthod. Dentofac. Orthop.* 159 (6), 799–807. doi:10.1016/j.ajodo.2020.02.024
- De Ridder, L., Aleksieva, A., Willems, G., Declerck, D., and Cadenas de Llano-Pérula, M. (2022). Prevalence of orthodontic malocclusions in healthy children and adolescents: a systematic review. *Int. J. Environ. Res. Public Health.* 19 (12), 7446. doi:10.3390/ijerph19127446

Data availability statement

The original contributions presented in the study are included in the article/supplementary material, further inquiries can be directed to the corresponding author.

Ethics statement

The studies involving humans were approved by Ethics Committee of Stomatology Hospital Affiliated to College of Stomatology of Dalian Medical University. The studies were conducted in accordance with the local legislation and institutional requirements. Written informed consent for participation in this study was provided by the participants' legal guardians/next of kin.

Author contributions

JZ methodology, investigation, formal analysis, data curation, writing original draft. CL investigation, data curation. YD conceptualization, supervision, project administration, reviewing and editing. All authors contributed to the article and approved the submitted version.

Acknowledgments

The authors acknowledge the participants who generously gave their help on the study.

Conflict of interest

The authors declare that the research was conducted in the absence of any commercial or financial relationships that could be construed as a potential conflict of interest.

Publisher's note

All claims expressed in this article are solely those of the authors and do not necessarily represent those of their affiliated organizations, or those of the publisher, the editors and the reviewers. Any product that may be evaluated in this article, or claim that may be made by its manufacturer, is not guaranteed or endorsed by the publisher.

- Duanmu, Z., Liu, L., Deng, Q., Ren, Y., and Wang, M. (2021). Development of a biomechanical model for dynamic occlusal stress analysis. *Int. J. Oral Sci.* 13 (1), 29. doi:10.1038/s41368-021-00133-5
- Farronato, G., Maspero, C., Esposito, L., Briguglio, E., Farronato, D., and Giannini, L. (2011). Rapid maxillary expansion in growing patients. Hyrax versus transverse sagittal maxillary expander: a cephalometric investigation. *Eur. J. Orthod.* 33 (2), 185–189. doi:10.1093/ejo/cjq051
- Fernandes, L. C., Farinazzo Vitral, R. W., Noritomi, P. Y., Maximiano, G. S., and José da Silva Campos, M. (2021). Influence of the hyrax expander screw position on displacement and stress distribution in teeth: a study with finite elements. *Am. J. Orthod. Dentofac. Orthop.* 160 (2), 266–275. doi:10.1016/j.ajodo.2020.04.031
- Fricke-Zech, S., Gruber, R. M., Dullin, C., Zapf, A., Kramer, F. J., Kubein-Meesenburg, D., et al. (2012). Measurement of the midpalatal suture width. *Angle Orthod.* 82 (1), 145–150. doi:10.2319/040311-238.1
- Garg, D., Rai, P., Tripathi, T., and Kanase, A. (2023). Effects of different force directions of intra-oral skeletally anchored maxillary protraction on craniomaxillofacial complex, in Class III malocclusion: a 3D finite element analysis. *Dent. Press J. Orthod.*, 5e2220377, 27. doi:10.1590/2177-6709.27.5.e2220377.oar
- Ge, Y. S., Liu, J., Chen, L., Han, J. L., and Guo, X. (2012). Dentofacial effects of two facemask therapies for maxillary protraction. *Angle Orthod.* 82(6):1083–1091. doi:10.2319/012912-76.1
- Kamath, A., Sudhakar, S. S., Kannan, G., Rai, K., and Sb, A. (2022). Bone-anchored maxillary protraction (BAMP): a review. *J. Orthod. Sci.* 11, 8. doi:10.4103/jos.jos_153_21
- Kojima, Y., and Fukui, H. (2006). A numerical simulation of tooth movement by wire bending. *Am. J. Orthod. Dentofac. Orthop.* 130 (4), 452–459. doi:10.1016/j.ajodo.2005.01.028
- Lee, B. W. (1965). Relationship between tooth-movement rate and estimated pressure applied. *J. Dent. Res.* 44 (5), 1053. doi:10.1177/00220345650440051001
- Lee, H., Nguyen, A., Hong, C., Hoang, P., Pham, J., and Ting, K. (2016). Biomechanical effects of maxillary expansion on a patient with cleft palate: a finite element analysis. *Am. J. Orthod. Dentofac. Orthop.* 150 (2), 313–323. doi:10.1016/j.ajodo.2015.12.029
- Lee, N. K., and Baek, S. H. (2012). Stress and displacement between maxillary protraction with miniplates placed at the infrazygomatic crest and the lateral nasal wall: a 3-dimensional finite element analysis. *Am. J. Orthod. Dentofac. Orthop.* 141 (3), 345–351. doi:10.1016/j.ajodo.2011.07.021
- Li, X., Kang, T., Zhan, D., Xie, J., and Guo, L. (2020). Biomechanical behavior of endocrowns vs fiber post-core-crown vs cast post-core-crown for the restoration of maxillary central incisors with 1 mm and 2 mm ferrule height: a 3D static linear finite element analysis. *Med. Baltim.* 99 (43), e22648. doi:10.1097/MD.00000000000022648
- Lisson, J. A., and Kjaer, I. (1997). Location of alveolar clefts relative to the incisive fissure. *Cleft Palate Craniofac J.* 34 (4), 292–296. doi:10.1597/1545-1569_1997_034_0292_loacr2_3.co_2
- Lombardo, G., Vena, F., Negri, P., Pagano, S., Barilotti, C., Paglia, L., et al. (2020). Worldwide prevalence of malocclusion in the different stages of dentition: a systematic review and meta-analysis. *Eur. J. Paediatr. Dent.* 21 (2), 115–122. doi:10.23804/ejpd.2020.21.02.05
- Maheshwari, A., Chawda, D. N., Kushwah, A., Agarwal, R. K., Golwara, A. K., and Dixit, P. B. (2023). Comparative evaluation of displacement and stress distribution pattern during mandibular arch distalization with extra and inter-radicular mini-implants: a three-dimensional finite element study. *Dent. Press J. Orthod.*, e2321373, 28. doi:10.1590/2177-6709.28.2.e2321373.oar
- Maspero, C., Cavagnetto, D., Fama, A., Giannini, L., Galbiati, G., and Farronato, M. (2020). Hyrax versus transverse sagittal maxillary expander: an assessment of arch changes on dental casts. A retrospective study. *Saudi Dent. J.* 32 (2), 93–100. doi:10.1016/j.sdentj.2019.06.003
- Matsumoto, K., and Tanna, N. (2021). Maxillary protraction and vertical control utilizing skeletal anchorage for midfacial-maxillary deficiency. *Dent. Press J. Orthod.*, e2120114, 26. doi:10.1590/2177-6709.26.6.e2120114.oar
- Mitani, Y., Choi, B., and Choi, J. (2018). Anterosuperior protraction of maxillae using the extraoral device, RAMP; finite element method. *Comput. Methods Biomech. Biomed. Engin* 21 (13), 722–729. doi:10.1080/10255842.2018.1514498
- Sadeghi, S., Hedayati, Z., and Mousavi-Fard, B. (2019). Comparison of two asymmetric headgear force systems: a finite element analysis. *Dent. Press J. Orthod.* 24 (2), 41.e1–41.e6. doi:10.1590/2177-6709.24.2.41.e1-6.onl
- Serpe, L. C. T., Torres, L. A. G., de Freitas Pinto, R. U., Toyofuku, A. C. M. M., and de Las Casas, E. B. (2014). Maxillary biomechanical study during rapid expansion treatment with simplified model. *J. Med. Imaging Health Inf.* 4 (1), 137–141. doi:10.1166/jmhi.2014.1233
- Shyagali, T. R., Patidar, R., Gupta, A., Kapoor, S., and Tiwari, A. (2023). Evaluation of stresses and displacement in the craniofacial region as a reaction to bone-anchored maxillary protraction in conjugation with posterior bite plane and rapid maxillary expansion in patients with Class III malocclusion: a finite element analysis study. *Am. J. Orthod. Dentofac. Orthop.* 164 (2), 253–264. doi:10.1016/j.ajodo.2022.12.015
- Somaskandhan, A., Kumar, N. M. V., and Vijayalakshmi, R. D. (2023). Stress distribution and displacement in the maxillofacial complex during intrusion and distalization of the maxillary arch using miniplates versus mini-implants: a 3-dimensional finite element study. *Prog. Orthod.* 24 (1), 8. doi:10.1186/s40510-023-00455-6
- Staminc, M., Marshall, G. W., Hilton, J. F., Pashley, D. H., Gansky, S. A., Marshall, S. J., et al. (2002). Ultimate tensile strength of dentin: evidence for a damage mechanics approach to dentin failure. *J. Biomed. Mater. Res.* 63 (3), 342–345. doi:10.1002/jbm.10230
- Sujaritanid, K., Suzuki, B., and Suzuki, E. Y. (2021). Comparison of one versus two maxillary molars distalization with iPanda: a finite element analysis. *Prog. Orthod.* 22 (1), 12. doi:10.1186/s40510-021-00356-6
- Tanaka, O. M., Araújo, E. A., Oliver, D. R., and Behrents, R. G. (2015). A finite element analysis of the maxillary first molar PDL with maxillary protraction in a mixed dentition Class III malocclusion. *Orthod. Craniofac Res.* 18 (4), 242–250. doi:10.1111/ocr.12102
- Trevizan, M., Nelson Filho, P., Franzolin, S. O. B., and Consolaro, A. (2018). Premaxilla: up to which age it remains separated from the maxilla by a suture, how often it occurs in children and adults, and possible clinical and therapeutic implications: study of 1,138 human skulls. *Dent. Press J. Orthod.* 23 (6), 16–29. doi:10.1590/2177-6709.23.6.016-029.oim
- Vracar, T. R., Claro, W., Vracar, M. E., 2nd, Jenkins, R. S., Bland, L., and Dayeh, A. A. (2021). Sutural deformation during bone-anchored maxillary protraction. *J. Oral Biol. Craniofac Res.* 11 (3), 447–450. doi:10.1016/j.jocr.2021.05.008
- Wang, J., Yang, Y., Wang, Y., Zhang, L., Ji, W., Hong, Z., et al. (2022). Clinical effectiveness of different types of bone-anchored maxillary protraction devices for skeletal Class III malocclusion: systematic review and network meta-analysis. *Korean J. Orthod.* 52 (5), 313–323. doi:10.4041/kjod.21.264
- Weinstein, A. M., Klawitter, J. J., and Cook, S. D. (1980). Implant-bone interface characteristics of bioglass dental implants. *J. Biomed. Mater. Res.* 14 (1), 23–29. doi:10.1002/jbm.820140104
- Woo, J. K. (1949). Ossification and growth of the human maxilla, premaxilla and palate bone. *Anat. Rec.* 105 (4), 737–761. doi:10.1002/ar.1091050408
- Zarrati, S., Bahrani, M., Heidari, F., and Kashani, J. (2015). Three dimensional finite element analysis of distal abutment stresses of removable partial dentures with different retainer designs. *J. Dent. (Tehran)* 12 (6), 389–397.
- Zhang, J. N., Lu, H. P., Hou, J., Wang, Q., Yu, F. Y., Zhong, C., et al. (2023). Deep learning-based prediction of mandibular growth trend in children with anterior crossbite using cephalometric radiographs. *BMC Oral Health* 23 (1), 28. doi:10.1186/s12903-023-02734-4